Valence fluctuation in ultrasmall CeO_2 nanoparticles

The size-dependent properties of nanoparticles have been intensively studied to better understand and utilize the unique behaviors of materials. Recently, ultra-small particles (i.e., approximately < 5 nm) have attracted attention because of their distinct characteristics compared to larger particles. Nanoparticles usually have distorted lattice structures depending on their particle size, which significantly affect their material properties [1,2]. These distortions vary depending on the material systems [3]. For example, the distortion of metals and metal oxides usually shows different tendencies for nanosizing; that is, lattice shrinkage occurs for metals and lattice expansion occurs for metal oxides [3]. The chemical state of oxygen plays a key role in the formation of nanoparticles.

While ultrasmall particles have been studied primarily for metals, investigations into ultrasmall metal oxides have been limited due to challenges in synthesis. Recently, ultrasmall metal oxides ranging from 1.5 nm have been successfully synthesized using a continuous-flow hydrothermal method with *in situ* surface organic modification [4], which opened a new research field of ultrasmall metal oxides [4,5]. This study presents the valence fluctuation phenomena observed in ultrasmall CeO_2 nanoparticles. Previously, for CeO_2 nanoparticles, research focused on the formation of oxygen vacancies, as redox properties are key for their application as solid catalysts. However, the intrinsic size effects without oxygen vacancy-related phenomena are not sufficiently understood.

The distortion and corresponding chemical states of ultrasmall CeO_2 were studied using high-energy-resolution fluorescence-detected X-ray absorption near-edge structure (HERFD-XANES) at SPring-8 **BL39XU**, X-ray absorption spectroscopy (XAS) and resonant inelastic X-ray scattering (RIXS) at SPring-8 **BL27SU**. Figure 1(a) shows the Ce L_3-edge HERFD-XANES spectra of CeO_2 nanoparticles. Peak A, which reflects the transition of Ce electrons from the 2*p* orbital to the 4*f* orbital, appears at 5721.9 eV for all the synthesized CeO_2 nanoparticles, suggesting that the valence of Ce in all the nanoparticles is predominantly +4. The splitting of peaks B_1, B_2, C_1, and C_2 based on the dipole transition from Ce $2p_{3/2}$ to $5d_{5/2}$ was affected by the crystal field in the CeO_2 fluorite structure, where the Ce atoms were surrounded by eight O atoms (O_h point group). Peaks based on crystal-field splitting were observed even at a grain size of 2.0 nm, indicating that the fluorite-type structure was maintained, although the peak splitting became less distinct with decreasing grain size.

Figure 1(b) shows the O *K*-edge XAS spectra of the ultrasmall CeO_2 (BL27SU). The three peaks between 530 and 545 eV were assigned to the interactions of O 2*p* with Ce 4*f*, Ce 5*d*-e_g, and Ce 5*d*-t_{2g}. With decreasing particle size, the peaks of O 2*p*–Ce 5*d*-e_g and O 2*p*–Ce 5*d*-t_{2g} were broadened, indicating disordering of the O atom positions. The CeO_2 nanoparticles contain few O vacancies; in turn, O displacement occurs within the framework of the fluorite structure. Furthermore,

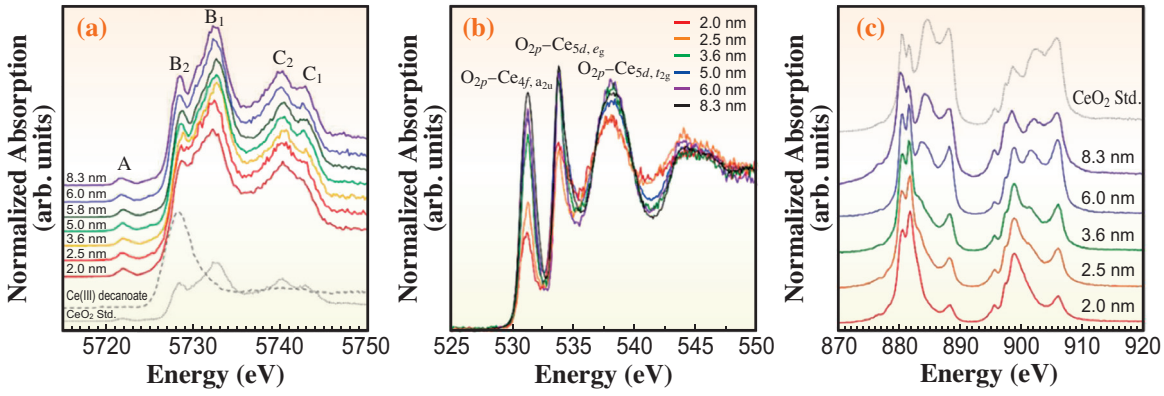

Fig. 1. X-ray absorption spectra of ultrasmall CeO_2 with different particle sizes. **(a)** Ce L_3-edge HERFD-XANES spectra. Ce(III) decanoate and purchased CeO_2 (Aldrich) were used as references. **(b)** O *K*-edge, and **(c)** Ce $M_{5,4}$-XAS profiles. [4]

the intensity of the O 2*p*–Ce 4*f* peak diminishes with decreasing particle size, particularly for particles smaller than 3 nm. This change likely results from reduced O 2*p*–Ce 4*f* hybridization. As shown in Fig. 1(c), the $M_{5,4}$-edge XAS spectra differs significantly from the Ce L_3-edge spectra (Fig. 1(a)) with respect to the appearance of Ce^{3+}, and the changes in the $M_{5,4}$-edge XAS spectra correspond to changes in the O states observed at approximately <3 nm.

Figures 2(a) and 2(b) show the RIXS map data for the Ce $M_{5,4}$-edges of CeO_2 with different particle sizes. The emission line starting at 874 eV is attributed to charge–transfer transitions with the hybridization of the valence electronic states of the 4*f* electrons and O ions. In Fig. 2(c), the Ce M_5 pre-edge (878.4 eV) was set as the excitation energy to investigate the grain-size dependence of the Ce $M_{5,4}$-edge RIXS spectrum. The peak intensity at loss energies of –7 to –4 eV decreases as the particle size decreases. This energy loss corresponds to a charge–transfer transition, which weakens the interaction between Ce 4*f* and O 2*p* as the particle size decreases. According to the L_3- and $M_{5,4}$-edge XAS spectra, the 4*f* electrons were localized in the <3 nm particles, irrespective of O vacancies, leading to the strong appearance of Ce^{3+} in the $M_{5,4}$-edge XAS spectra, but not in the L_3-edge and XAS spectra. Note that the existence of Ce^{3+} in the ultrasmall particles was caused by distortion rather than oxygen release. The local structure of the CeO_8 hexahedra became more disordered with the weakening of the O–Ce interaction and the localization of the 4*f* electrons. The ultrasmall CeO_2 nanoparticles here exhibit a distinctive electronic state with valence fluctuations due to their large lattice expansion/distortion, maintaining high crystallinity and oxidation state.

Ultrasmall metal oxides with unusual electronic states have great potential for exploiting new properties in the future, where the synthesis method is applicable to various metal oxides, including mixed oxides [4,5].

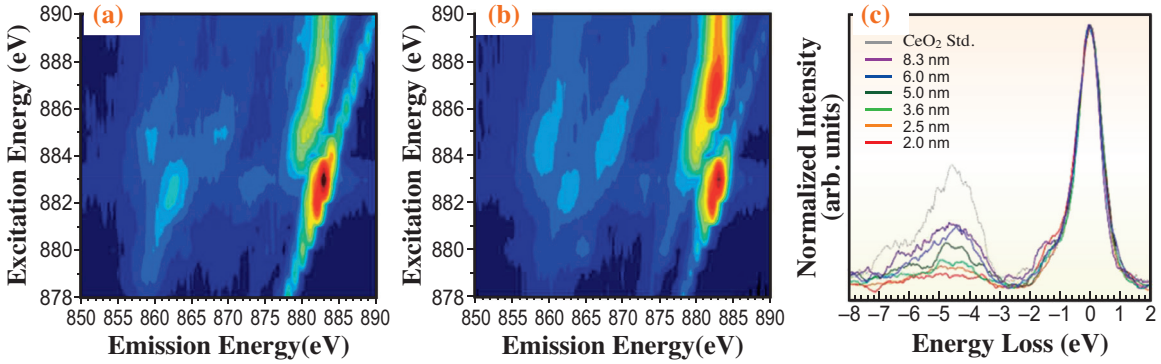

Fig. 2. Ce M_5-edge RIXS maps of CeO_2 nanoparticles with sizes of **(a)** 2.0 and **(b)** 6.0 nm. The fluorescence at 855–875 eV was attributed to $5p \rightarrow 3d$ emission and the Coster–Kronig transition ($3d_{5/2} \rightarrow 3d_{3/2}$ emission). **(c)** Ce M_5-edge RIXS spectra of CeO_2 nanoparticles of different sizes. The incident X-ray energy was set to 878.4 eV. [4]

Akira Yoko[a,b,*], Kakeru Ninomiya[a] and Maiko Nishibori[a,c]

[a] International Center for Synchrotron Radiation Innovation Smart, Tohoku University
[b] WPI-Advanced Institute for Materials Research, Tohoku University
[c] Institute of Multidisciplinary Research for Advanced Materials, Tohoku University

*Email: akira.yoko.c7@tohoku.ac.jp

References

[1] X. Hao *et al.*: Small **14** (2018) 1802915.
[2] X. Hao *et al.*: Acta Mater. **203** (2021) 116473.
[3] P. M. Diehm *et al.*: ChemPhysChem **13** (2012) 2443.
[4] *A. Yoko, Y. Omura, K. Ninomiya, M. Nishibori, T. Fujita, H. Kasai, E. Nishibori, N. Chiba, G. Seong, T. Tomai, T. Adschiri: J. Am. Chem. Soc.* ***146*** *(2024) 16324.*
[5] C. Han *et al.*: Chem. Eng. J. **496** (2024) 154022.